ELSEVIER

Nuclear magnetic resonance spectral analysis and conformational properties of 11-benzoyl-9,9a,10,11-tetrahydro-4H-indolo[4,3-ab]carbazole

T. Mavromoustakos [a],*, I.K. Stamos [b], C. Kamoutsis [b], E. Theodoropoulou [a], M. Zervou [a], E. Humpfer [c]

[a] *Institute of Organic and Pharmaceutical Chemistry, The National Hellenic Research Foundation, Vas. Constantinou Ave. 48, 11635 Athens, Greece*
[b] *School of Health Sciences, Department of Pharmacy, University of Patras, Rion, Patras 26500, Greece*
[c] *Bruker Analytische Messtechnik GMBH, Wikingerstr. 13, D-76189 Karlshruhe, Germany*

Abstract

The structure of 11-benzoyl-9,9a,10,11-tetrahydro-4H-indolo [4,3-ab] carbazole, a candidate molecule to possess significant antitumor or antimicrobial activity, was elucidated using a combination of one-dimensional and two-dimensional nuclear magnetic resonance (NMR) techniques. Its conformational properties were studied using a combination of two-dimensional NOESY spectroscopy and molecular modeling. Such information will be of aid to synthetic chemists who aim to develop derivatives of this structure. It may also provide information about the stereoelectronic requirements that govern their activities. © 1998 Elsevier Science B.V.

Keywords: 11-Benzoyl-9,9a,10,11-tetrahydro-4H-indolo[4,3-ab]carbazole; Molecular modeling; Nuclear magnetic resonance spectrometry

1. Introduction

Functionalized benzo[a]- and [b]-anellated carbazoles are pharmacologically important structures since such compounds possess interesting biological properties, particularly cytostaticity [1–3] and antimicrobial activity [4].

Certain derivatives of their nitrogen analogs, namely pyridino[b]-anellated carbazoles, commonly referred to as ellipticine alkaloids (**I**) are being used clinically to inhibit the growth of several human tumors. In fact, one such derivative has been used in the therapy of kidney, breast and thyroid cancer [5]. The mechanism of action of these benzo- and pyridino-carbazoles involves intercalation into DNA.

Furthermore, certain indolo-anellated carbazoles (**II**), with an amido group attached to them, constitute the aglycon moiety of recently discov-

---

* Corresponding author. Tel.: + 30 1 7253821; fax: + 30 1 7253821/7247913.

ered antibiotics, which have been isolated from various soil organisms, blue–green algae and slime molds. This family of natural products, commonly known as the indolocarbazole alkaloids, also possesses interesting and diverse biological activities [6].
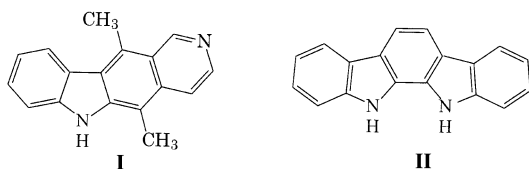
An outstanding member of this group of natural products is the glycoside staurosporine which displays bis-*N*-glycosidic linkages, and a nanomolar protein kinase C inhibitory activity [7].

Protein kinase C (PKC) is a family of phosphorylating isoenzymes which play a key role in several crucial cellular processes such as signal transduction, cell differentiation and cell growth. The discovery that tumor-promoting phorbol diesters (potent co-carcinogens) function by activating PKC infers that inhibitors of PKC might serve as anticancer agents.

Rebeccamycin, with only one glycosidic linkage is another representative of a subclass in indolocarbazoles which serves to illustrate both bioactivity and structural diversity. The recent finding that this subclass of antibiotics can bind to DNA has led rebeccamycin in the late stage of clinical evaluation as an anticancer agent [8,9].

Tjipanazoles, which are desamido analogs of rebeccamycin, except for the tjipanazole J, and are microbial products also, exhibit antifungal as well as antitumor activity. On these considerations, the aglycon moiety (**II**) constitutes a major structural unit of many of the indolocarbazole microbial products.

In this article, the structural assignments and conformational properties of a novel indolocarbazole molecule (**III**), where the two nitrogen atoms have lost their proximity, are presented. Moreover, one is an indolic nitrogen atom while

the other one is an indolinic nitrogen atom, protected with a benzoyl group.
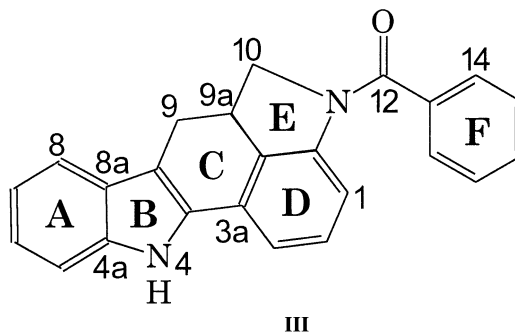
$$\tau 1 \quad C14\text{-}C13\text{-}C12\text{-}O19$$
$$\tau 2 \quad C13\text{-}C12\text{-}N11\text{-}C10$$

2. Materials and methods

2.1. Sample preparation

The sample for high-resolution nuclear magnetic resonance (NMR) experiments consisted of 11-benzoyl-9,9*a*,10,11-tetrahydro-4H-indolo[4,3-*ab*]carbazole, dissolved in deuterated DMSO (5 mg in 0.4 ml) with TMS used as the chemical shift reference. The 11-benzoyl-9,9*a*,10,11-tetrahydro-4H-indolo[4,3-*ab*]carbazole was synthesized in our laboratory. Details of its synthesis will be given in a subsequent study.

2.2. NMR spectroscopy

The high-resolution NMR experiments were performed on a DRX 500 MHz spectrometer equipped with a 5 mm inverse triple resonance probe with a *z*-gradient. The only DEPT experiment was run with an AC 300 MHz spectrometer. All data were collected using pulse sequence and phase-cycling routines provided in the Bruker library of pulse programs. Data processing, including sine-bell apodization, Fourier transformation and plotting, were performed using Bruker software packages. ^{1}H-NMR spectra were recorded using the following acquisition parameters: 90° pulse width (PW) 11.0 μs, spectral width (SW)
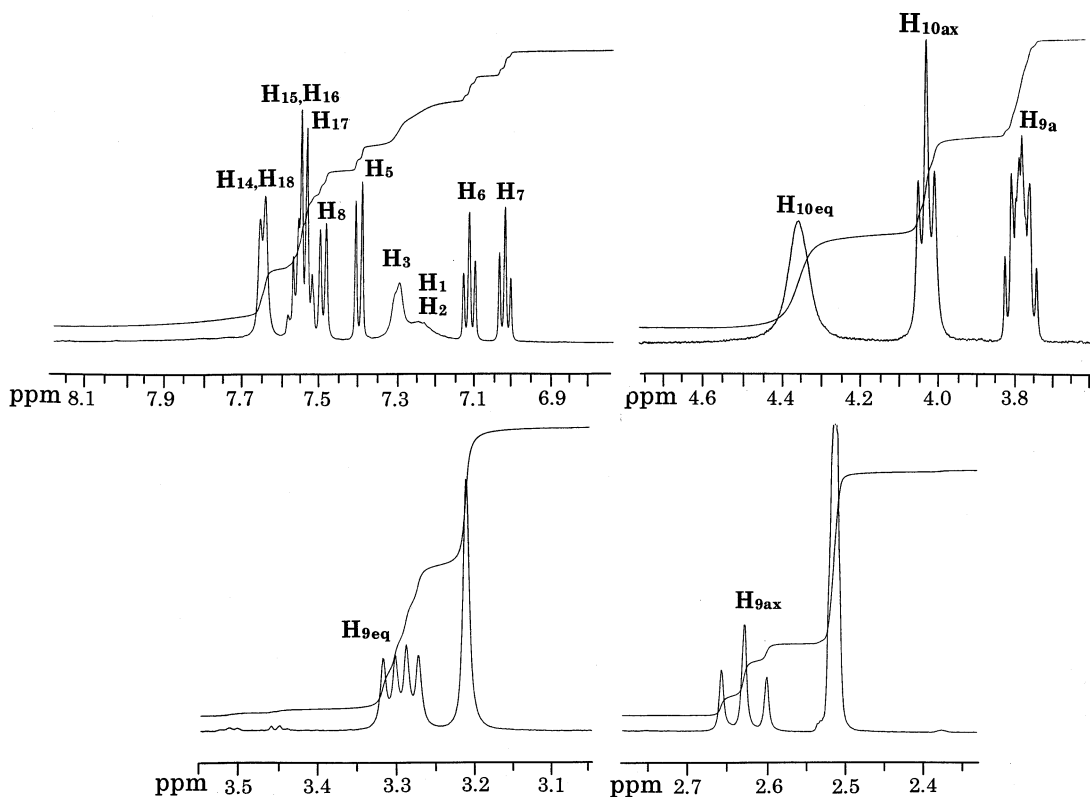
Fig. 1. ^{1}H-NMR spectrum of 11-benzoyl-9,9a,10,11-tetrahydro-4H-indolo [4,3-*ab*]carbazole in DMSO at 298 K recorded on a Bruker DRX 500 MHz.

10 330 Hz, data size (TD) 32K, recycling delay (RD) 2.0 s, number of transients (NS) 8, and free induction decay (FID) resolution 0.32 Hz per point (Hz pt^{-1}). ^{13}C-NMR spectra were performed with PW 8.4 μs, SW 131 579 Hz, TD 16K, RD 9.4 s, NS 512 and digital resolution 0.803 Hz pt^{-1}. The ^{1}H–^{1}H correlation COSYGS spectrum was obtained with recycling delay (D1) 1.5 s, D0 increment 3 μs, spectral width in F_2 11.16 ppm and in F_1 11.16 ppm. The data sizes were 128 W and 2K in F_1 and F_2, respectively. The FID resolution for F_1 was 43.6 Hz pt^{-1} and in F_2 was 2.72 Hz pt^{-1}. A two-dimensional (2D) ^{1}H–^{1}H nuclear Overhauser enhancement spectrum was recorded using: D1 = 2.0 s, D0 = 3 μs, SW in both F_2 and F_1 was 13.02 ppm. FID resolution was 3.18 Hz pt^{-1} in F_2 and 12.72 Hz pt^{-1} in F_1. The various ^{13}C directly coupled to one proton were assigned using an inverse corre-

lation experiment with gradients. This phase-sensitive experiment was run at 325 K using the following acquisition parameters: data size in F_2 1K and in F_1 128 W. The spectral width used in F_1 was 167 ppm and in F_2 11.16 ppm. The FID resolution in F_1 was 164.13 Hz pt^{-1} and in F_2 5.45 Hz pt^{-1}. The number of transients used was 4 and there were 8 dummy scans. The inverse long-range correlation experiment (INV4GSLPKRND) with gradients was performed using a low pass filter at 325 K and the following acquisition parameters: data size in F_2 2K and in F_1 128 W. The spectral width used in F_1 was 222.095 ppm and in F_2 11.16 ppm. The FID resolution in F_1 was 218.23 Hz and in F_2 2.72 Hz. The ^{1}H–^{13}C long-range correlations were obtained with recycling delay of 1.5 s and D0 increment of 3 μs. The number of transients used was 8 and there were 16 dummy scans.
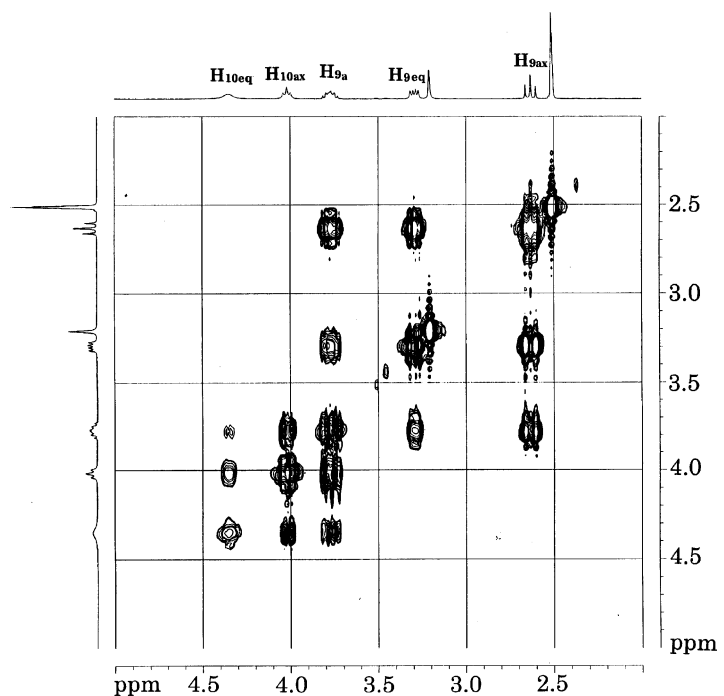
Fig. 2. 2D COSYGS spectrum of an expanded area 2–4.6 ppm of 11-benzoyl-9,9a,10,11-tetrahydro-4H-indolo[4,3-*ab*]carbazole in DMSO at 298 K recorded on a Bruker DRX 500 MHz.
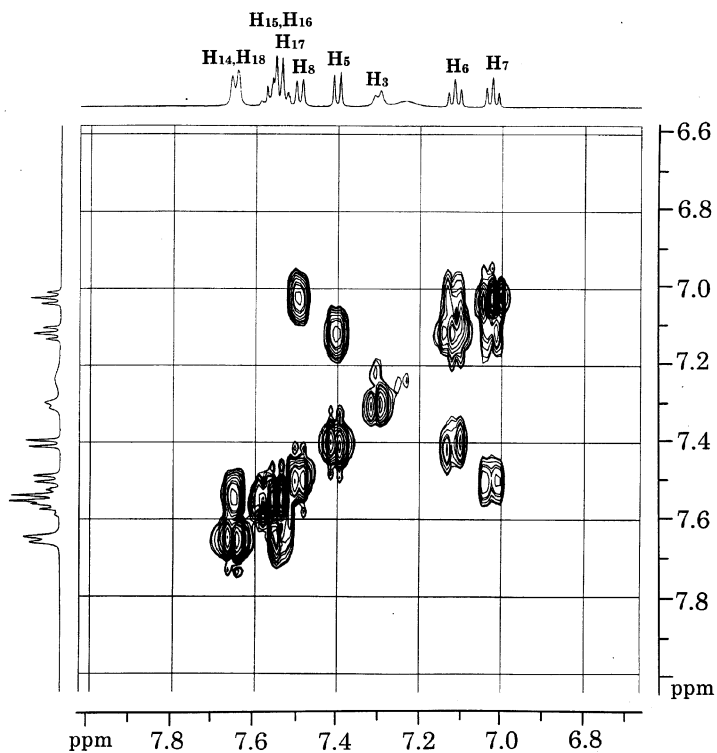

Fig. 3. 2D COSYGS spectrum of an expanded area of 6.6–7.9 ppm of 11-benzoyl-9,9a,10,11-tetrahydro-4H-indolo[4,3-*ab*]carbazole in DMSO at 298 K recorded on a Bruker DRX 500 MHz.

2.3. Molecular modeling

Computer calculations were performed on a Silicon Graphics 4D/35 using the QUANTA 3.3 version. The energy of the compound was first minimized. The low-energy conformer was then subjected to exhaustive grid search conformational analysis around τ_1 and τ_2 dihedral angles. The increments used for both dihedral angles were 10°. Thus, $36 \times 36 = 1296$ conformers were generated. The contour plot included only energy levels that differed by as much as 10 kcal mol^{-1} from the lowest energy level. Conformers picked from the different low energy levels were further energy minimized. Details of these techniques are described in our previous publications [10,11].

3. Results and discussion

3.1. Structure elucidation

The ^{1}H-NMR spectrum of the studied compound is shown in Fig. 1. Identification of individual peaks in the ^{1}H-NMR spectrum was obtained by peak integration and from the 2D-NMR correlation spectroscopy with gradients (COSYGS) experiment. The proton resonated at 2.63 ppm was assigned as H9$_{ax}$ because it has an axial vicinal coupling approximately equal to the geminal coupling (15 Hz). Conversely, the proton resonated at 3.3 ppm was labelled H9$_{eq}$ because it shows a large geminal and a smaller vicinal couplings. Peaks due to H1 and H3 are broad because of their extended conjugation with both indolic and indolinic nitrogens. Expanded regions of the COSYGS experiment are shown in Figs. 2 and 3.

The through space ^{1}H connectivities were obtained from the 2D ^{1}H–^{1}H nuclear Overhauser enhancement spectroscopy (NOESY) spectrum (Fig. 4). The nuclear Overhauser enhancement (NOE) cross-peaks that arise due to dipolar interactions give mainly essential information about the conformation of the molecule. Structural assignments can also be aided from the NOEs as shown in Fig. 4. The most important are due to the following proton pairs: NH–H3,

NH–H5, H8–H9$_{eq}$, and H9$_{ax}$–H10$_{ax}$. Of them, NOEs of NH–H3 and NH–H5 establish proximity of indolic NH with the two adjacent phenyl rings. NOE between H8 and H9$_{ax}$ indicates proximity of A and C rings of carbazole moiety. H9$_{ax}$–H10$_{ax}$ associates close proximity between C and E rings.

A ^{13}C distortionless enhancement by polarization transfer (DEPT) was run in order to assign the carbon chemical shifts (Fig. 5). Due to the complex patterns of the different kinds of carbons, the assignment was aided by other experiments. Thus, the assignment of CH carbons was achieved with an inverse ^{13}C–^{1}H NMR experiment (see Figs. 6 and 7). The tertiary carbons were assigned on an inverse long-range correlation experiment with gradients. This experiment aided the unambiguous assignment of H8–H5–H6–H7 group protons, as can be seen in Fig. 8. In addition, synthesis of simpler analogs confirmed the structural assignments. Details of the synthesis of these analogs will be given in a subsequent paper. In conclusion, the strategy used for the structure elucidation of the studied compound was to combine the information derived from ^{1}H- and ^{13}C-NMR spectra of the studied compound and other analogs of similar structure.

3.2. Conformational analysis

NOE data also aided the conformational analysis of the molecule studied. Thus, H10–H14 NOE establishes a spatial vicinity between E and F rings. This spatial close proximity between H10 and H14 is not obvious in the chemical structure of the studied molecule.

In order to further examine this observation, we performed grid search conformational analysis on the critical dihedral angles τ_1 and τ_2, using as a starting conformer the minimized structure of the studied molecule. This analysis provides the different potential energies that the combinations of these two dihedral angles can adopt. The energy levels which differed by as much as 10 kcal mol^{-1} from the lowest energy level may represent the most favored candidates for biological activity. The contour plot gener-

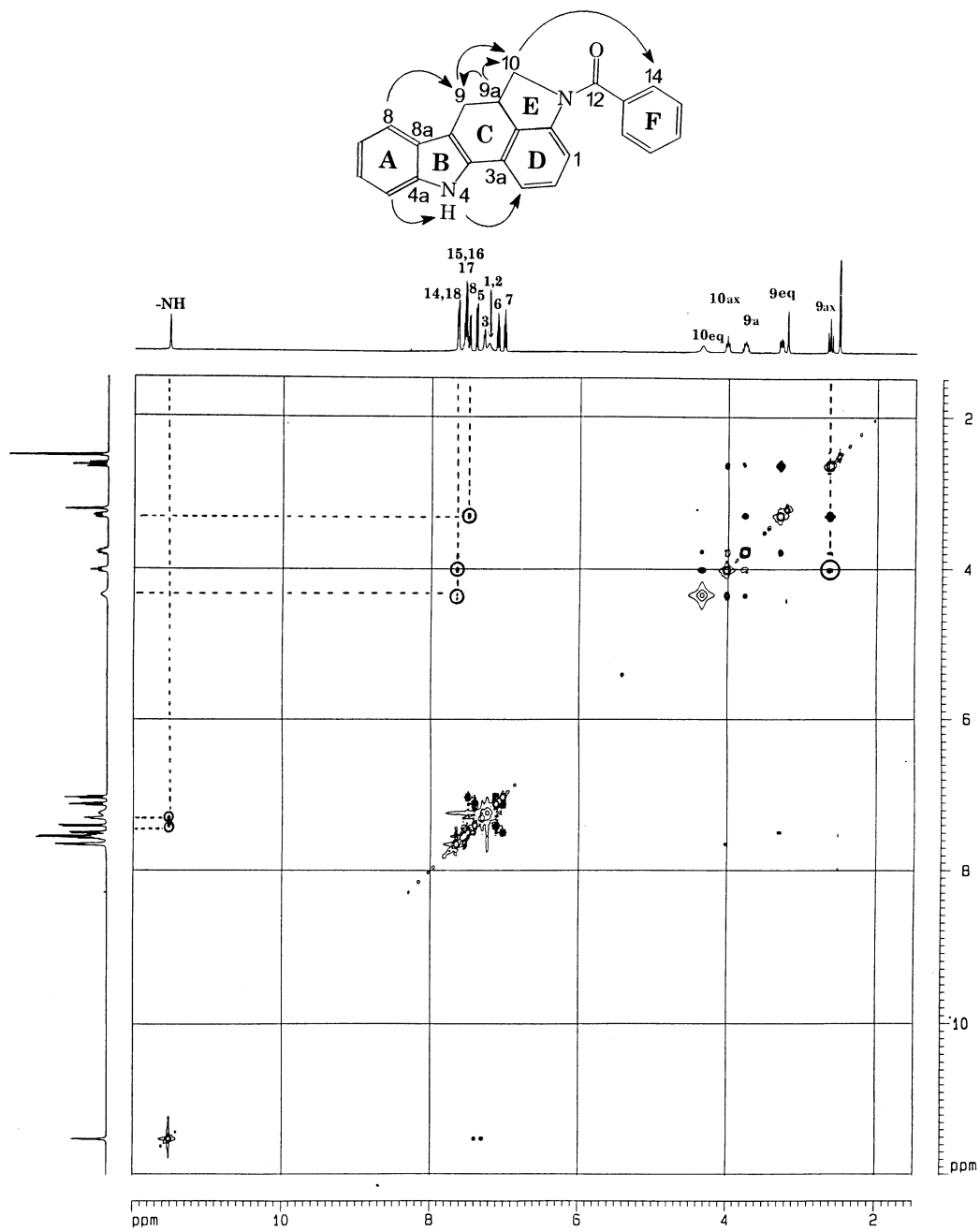Fig. 4. 2D phase-sensitive NOESY spectrum of 11-benzoyl-9,9a,10,11-tetrahydro-4H-indolo[4,3-ab]carbazole in DMSO at 298 K recorded on a Bruker DRX 500 MHz. The lines indicate the observed nuclear Overhauser enhancements due to through-space interproton couplings.
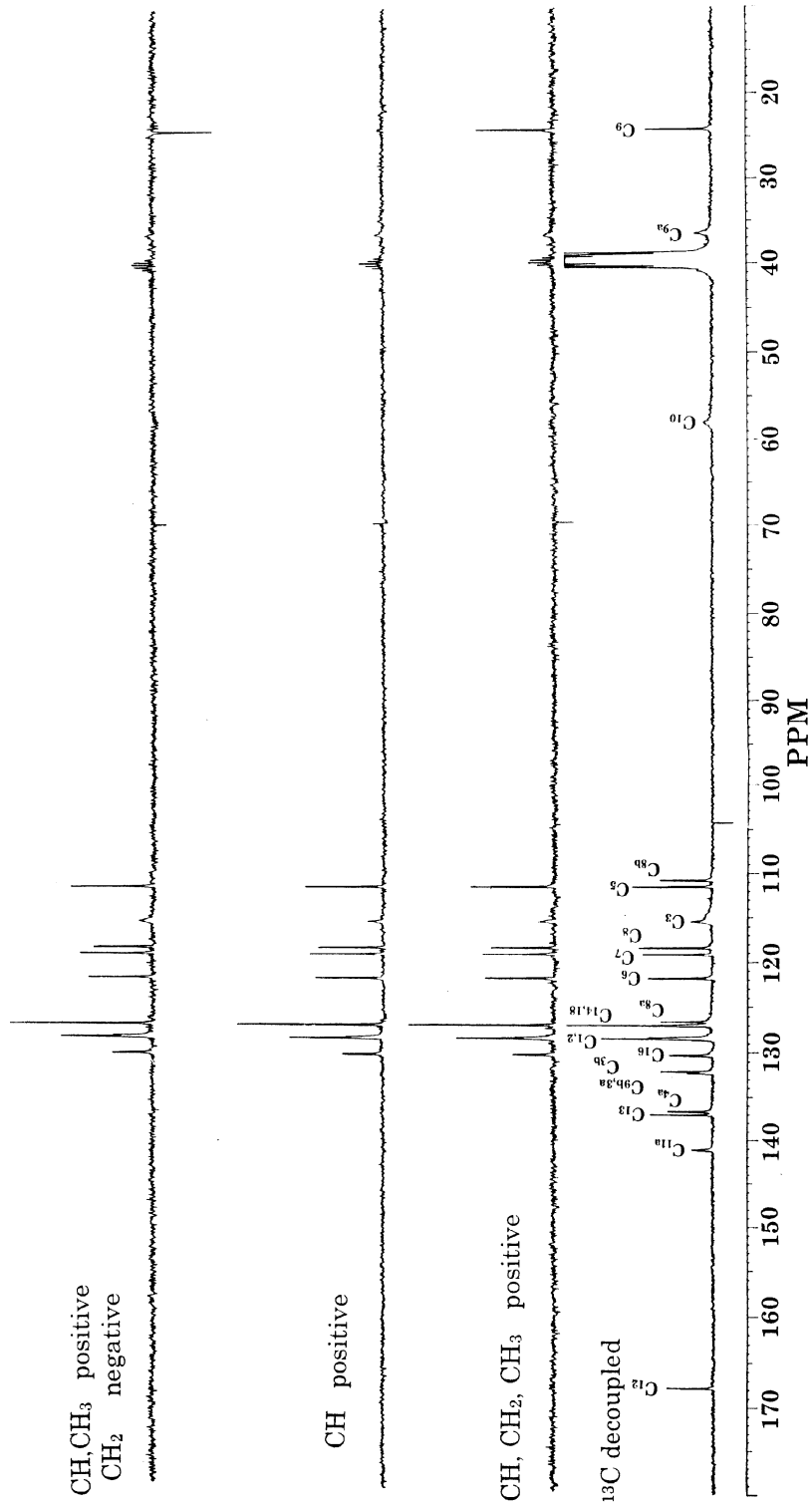
Fig. 5. ¹³C-NMR DEPT spectra of 11-benzoyl-9,9a,10,11-tetrahydro-4H-indolo [4,3-*ab*]carbazole in DMSO at 298 K recorded on a Bruker 300 AC.

Fig. 6. ^{13}C–^{1}H inverse correlation experiment of an expanded area of 2.0–4.55 ppm of of 11-benzoyl-9,9a,10,11-tetrahydro-4H-indolo[4,3-*ab*]carbazole in DMSO at 298 K recorded on a Bruker DRX 500 MHz.

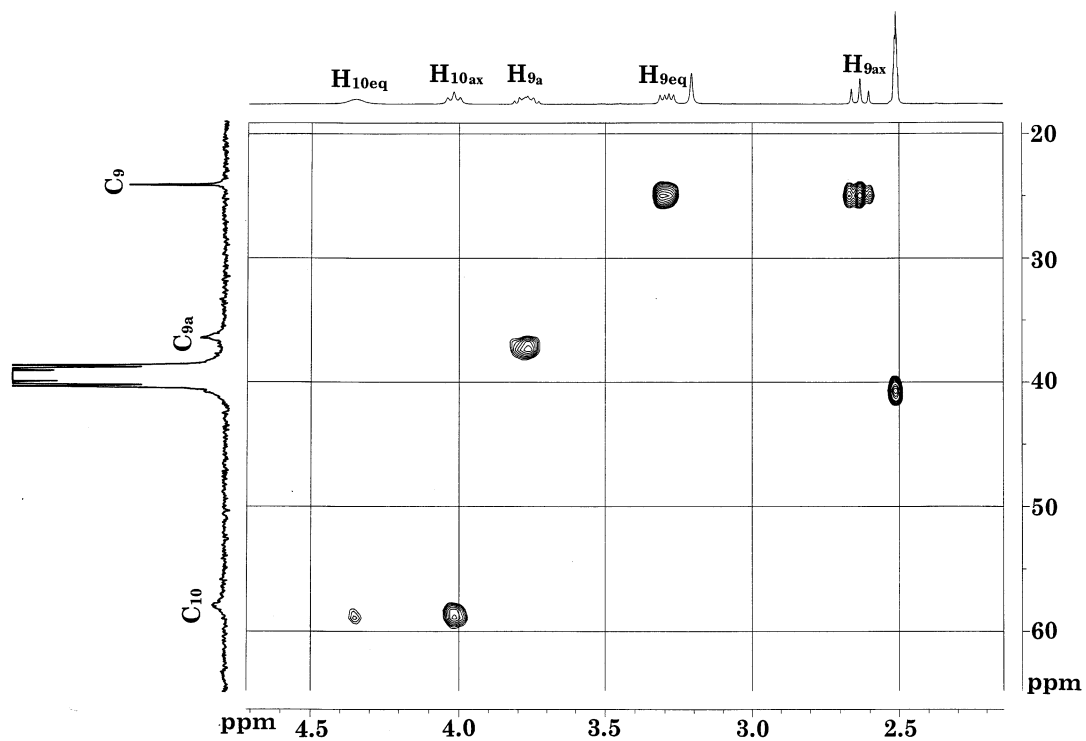Fig. 7. ^{13}C–^{1}H inverse correlation experiment of an expanded area of 6.7–8.0 ppm of 11-benzoyl-9,9a,10,11-tetrahydro-4H-indolo[4,3-*ab*]carbazole in DMSO at 298 K recorded on a Bruker DRX 500 MHz.
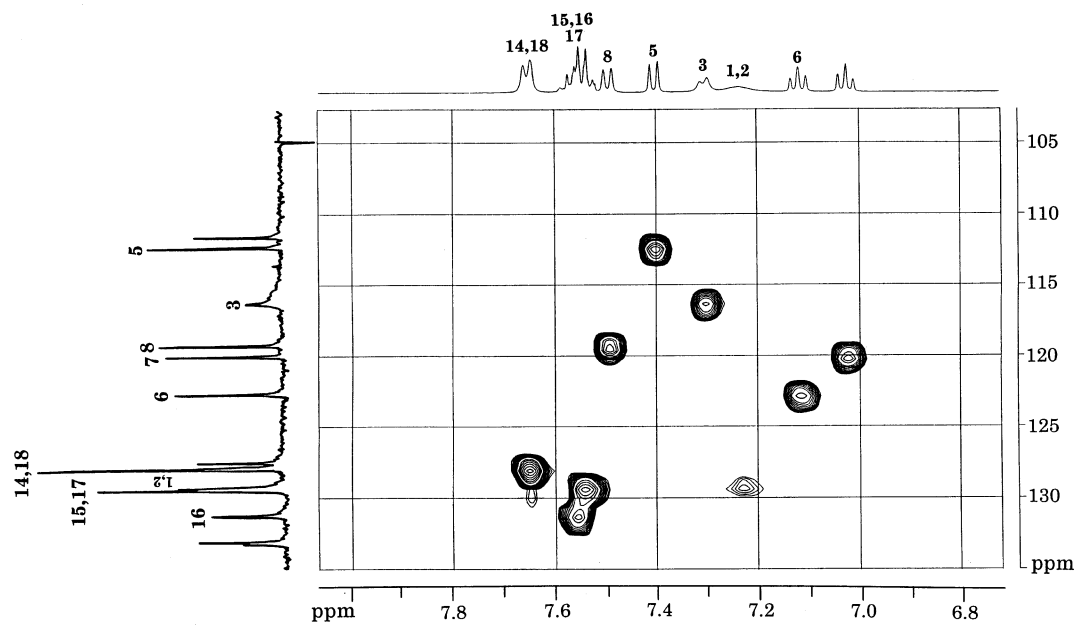
Fig. 8. ^{13}C–^1H long-range correlation experiment of 11-benzoyl-9,9a,10,11-tetrahydro-4H-indolo[4,3-*ab*]carbazole in DMSO at 325 K recorded on a Bruker DRX 500 MHz.

Fig. 9. Contour plot as a function of τ_1 and τ_2 dihedral angles of 11-benzoyl-9,9a,10,11-tetrahydro-4H-indolo[4,3-*ab*]carbazole obtained from a conformational grid search analysis with increments of 10°.

ated after incrementing both dihedral angles by 10^0 is shown in Fig. 9. The eight areas of low-energy contour levels observed contained energy levels which differed by as much as 10 kcal mol^{-1}

Table 1
Conformational descriptors for τ_1 and τ_2 dihedral angles generated in the grid search conformational analysis. The distance between H10–H14 protons was calculated in these conformers in an attempt to compare the theoretical calculations with the observed NOE experimental results

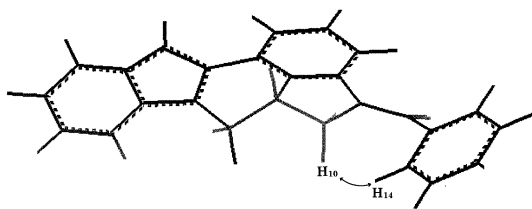| Conformers	τ_1	τ_2	H10–H14 (Å)
A	47.9	−131.8	2.902
B	100.0	1.7	5.011
C	104.4	−26.8	5.465
D	129.1	151.0	3.423
E	−127.6	−132.9	3.194
F	−93.4	5.9	5.018
G	−76.5	−23.7	5.468
H	−51.7	154.1	3.194

Fig. 10. A representative low-energy conformer of 11-benzoyl-9,9a,10,11-tetrahydro-4H-indolo[4,3-*ab*]carbazole that favors the observed NOE between H10–H14 protons.

Its conformational properties were studied using a combination of 2D NOESY experiment and molecular modeling techniques. The use of molecular modeling provided the conformational space available for its critical angles τ_1 and τ_2. Theoretical results pointed out the flexibility of the phenyl acetyl moiety in the molecule. This flexibility may play an important role in its biological activity.

from the lowest one. As can be observed, there are some combinations between τ_1 and τ_2 dihedral angles that are of high energy and do not fall within this limit. This is because at these dihedral angle combinations, the D and F phenyl rings are in an energetically unfavored close proximity. Low-energy conformers from the eight areas were selected and further minimized. Conformational descriptors of the conformers A–G as well as the calculating distance between H10 and H14 for these conformers are shown in Table 1. These theoretical calculations show that only some conformers favor the observed NOE. For example, conformer A favors such an observed NOE because the calculated distance between H10 and H14 is 2.9 Å (Fig. 10).

4. Conclusions

The combination of ¹H and ¹³C data resulted in the structure determination of 11-benzoyl-9,9a,10,11-tetrahydro-4H-indolo[4,3-*ab*]carbazole.

References

[1] A. Segall, H. Pappa, R. Causabon, G. Martin, R. Bergoc, M.T. Pizzorno, Eur. J. Med. Chem. 30 (1995) 165–169.

[2] U. Kuckländer, H. Pitzler, K. Kuna, Arch. Pharm. (Weinheim) 327 (1994) 137–142.

[3] A. Segall, H. Pappa, M.T. Pizzorno, M. Radice, A. Amoroso, G.O. Gutkind, Il Farmaco 51 (1996) 513–516.

[4] G.W. Gribble, in: A. Brossi (Ed.), The Ellipticine Alkaloids, The Alkaloids: vol. 39, Academic Press, New York, 1990, pp. 239-343.

[5] G.W. Gribble, S.J. Berthel, in: A.U. Rahman (Ed.), Studies in Natural Products Chemistry, vol. 12, Elsevier Science Publishers, Dordrecht, 1993, pp. 365-409.

[6] S. Omura, Y. Sasaki, Y. Iwai, H. Takeshima, J. Antibiotics 49 (1995) 535–548.

[7] B.S. Krishnan, M.E. Moore, C.P. Lavoie, B.H. Long, R.A. Dalterio, H.S. Wong, I.E. Rosenberg, J. Biomol. Struct. Dyn. 12 (1994) 625–636.

[8] Y. Yamashita, N. Fujii, C. Murkata, T. Ashizawa, M. Okabe, H. Nakano, Biochemistry 31 (1992) 12069–12075.

[9] F.G.Mann, A.J. Tetlow, J. Chem. Soc. (1957) 3352-3366.

[10] J. Matsoukas, J. Hondrelis, M. Keramida, R. Yamdagri, Q. Wu, T. Mavromoustakos, A. Makriyannis, G. Moore, J. Biol. Chem. 269 (1994) 5303–5312.

[11] T. Mavromoustakos, D.-P. Yang, E. Theodoropoulou, A. Makriyannis, Eur. J. Med. Chem. 30 (1995) 227–234.